Arabian Journal of Geosciences (2022) 15:1621
https://doi.org/10.1007/s12517-022-10864-2

ORIGINAL PAPER

Electromagnetic radiation characteristics of coal under multiple loading methods and its relationship with porosity

Qi Zhang[1] · Xiangchun Li[1] · Zhanwen Fan[2] · Mingxiu Xing[1] · Yinqing Wang[1] · Kedi Wang[1] · Yaoyu Shi[1]

Received: 17 November 2021 / Accepted: 11 September 2022 / Published online: 18 October 2022

Abstract

This study deploys cyclic loading and multi-stage loading methods to study the influence of the loading method on electromagnetic radiation (EMR) characteristics in the failure process of coal. For this purpose, these methods were applied to Sihe coal samples. The EMR signals were collected during the experiments. The varying relationship between the EMR characteristics of the loaded coal and the porosity was analyzed based on the porosity of coal samples measured by small-angle X-ray scattering (SAXS) experiments. The results indicated that the EMR signals magnify with the increase of axial stress and decline with the decrease of axial stress. The generation of the EMR pulse and amplitude under the multi-stage loading conditions is relatively smooth during the constant load stage, but the number of EMR pulses increases when the stress increases from one level to another. Moreover, the results indicated that the EMR characteristics and porosity changes are closely related to the opening, closing, and development state of pores and fractures inside the coal. These findings provide the means necessary to establish the relationship between the EMR pulse cumulative counting and the porosity of the loaded coal. During the failure process, the change in EMR pulses cumulative counting follows after the alteration in the porosity. The amount of change in both parameters reaches the maximum when the coal fails. The maximum cumulative counting of EMR pulses was 1,111,114 and 37,464 for cyclic and graded loading conditions, respectively. At the same time, the change of porosity of the loaded coal also reaches the maximum.

Keywords Electromagnetic radiation (EMR) · Cyclic loading · Multi-stage loading · Small-angle X-ray scattering (SAXS) · Porosity

Introduction

Energy consumption and production are important strategic concerns for developing and developed countries (Aydin and Tarverdian 2007; Aydin et al. 2014). Logical planning for the use of various energy sources is important in the context of global energy consumption (Aydin 2014, 2015). Coal is the main source of energy in China and will play an important role for a long time in the future of this country. With the depletion of shallow resources, China's coal resources have gradually entered the deep mining stage. The intensity and hazard degree of coal rock dynamic disaster accidents such as coal and gas outbursts and underground impact pressure restricts the safe production of coal mines. Improving the detection and early warning of protrusion and impact hazard areas is crucial to enhancing the level of dynamic disaster accident prevention and control.

The most alarming phenomenon before the occurrence of coal rock dynamic disasters is the failure and instability of the coal and rock mass. In this process, the internal energy of the rock mass and coal is released. For this reason, many technical means have been developed to monitor and analyze the physical parameters in the failure process of coal rock mass, which in turn facilitate an in-depth study of the failure process and mechanism of coal rock mass under different loading conditions (Wu et al. 2021; Dou et al. 2021; Li et al. 2022). Typical early warning methods for the outburst

Responsible Editor: Murat Karakus

✉ Xiangchun Li
chinalixc123@163.com

[1] School of Emergency Management and Safety Engineering, China University of Mining and Technology-Beijing, Haidian District, Ding No.11 Xueyuan Road, Beijing 100083, China

[2] CHN Energy Coal Coking Chemical Company, Ordos 016000, China

and dangerous impact areas mainly include drilling to evaluate gas base parameters (K1 values and S values, etc.) and monitoring parameters during gas extraction (Li et al. 2019a, b). However, these measures are mostly based on regular sampling or fixed-point indicators, which hardly reflect the regional stress environment of coal and rock mass in the dynamic process of mining due to the larger drilling quantities, higher cost, more subjective human factors, and discontinuous monitoring in the time domain. Energy is released in the form of elastic waves, electric charge, and electromagnetic radiation during the failure of coal rock mass, where all forms of energy release show certain regularities. Besides, there will be an abnormal and sudden change in energy levels before the failure of the coal rock mass. EMR monitoring technology is capable of capturing these changes and as a result, it has gradually become one of the effective means of monitoring the failure and stress state of coal rock mass (Ai et al. 2020; Hu et al. 2014; Dou et al. 2007). It has also become an important method used to prevent and control coal and rock dynamic disasters (Yuan et al. 2018; He et al. 2007; Sun et al. 2012).

Although the EMR monitoring and early warning technology is an effective non-contact method for coal rock dynamic hazards, it is mostly limited to the time and frequency domain description of EMR signals and does not account for the changes in porosity caused by deformation and failure in the coal rock mass. The fugacity and flow characteristics of CH4, CO2, and N2 in coal mass change due to the transformations induced in the pore structures (including micropores and mesopores structures) under the complex stress environments. In turn, the fugacity characteristics and flow characteristics of CH4, CO2, and N2 affect the fracture evolution patterns in the coal mass. The small-angle X-ray scattering (SAXS) experiment can record the scattering information of microscopic open pores in the material and the closed pores that cannot be otherwise determined by the fluid intrusion methods such as the pressure tribute method. In this way, the existence of all pore structures in the material can be covered (Melnichenko et al. 2012; Sakurovs et al. 2012). Besides, the SAXS experiment enables the quantitative analysis of porosity during loading, which provides the possibility to deeply analyze the relationship between electromagnetic radiation and porosity evolution. Moreover, due to the complex stress disturbance often encountered in the engineering coal rock mass, a variety of mechanical behaviors are intertwined and crossed. The stability of the coal rock mass structures deteriorates rapidly under the conditions of stress disturbance, and the coal rock dynamic hazards present complexity (Wang et al. 2021, 2022; Zhu et al. 2022). Therefore, studying the EMR characteristics of coal and rock mass under the coupling effects of cyclic loading and multi-stage loading can promote the development of EMR prediction technology and improve its accuracy.

Materials and methods

Sample preparation

The raw coal samples used in the experiments were collected from the Shihe coal mine, Jincheng City, China. They were hermetically sealed by anti-vibration foam to avoid collision-induced damage to the internal structures. After being sent to the laboratory, the raw coal samples were drilled and sampled immediately. When coring, the location where the primary fractures and defective structures are found should be avoided and the core must be drilled in the direction of parallel laminae. Subsequently, a standard cylindrical coal sample specimen with a length of 100 mm and a diameter of 50 mm was cut by a cutting machine, and then the samples were smoothed and polished at both ends according to the method recommended by the International Society for Rock Mechanics (ISRM), keeping the error of parallelism of the specimen ends less than 0.05 mm and the error of smoothness of the end surfaces less than 0.02 mm. The coal samples prepared in experiments are shown in Fig. 1.

The principles of the EMR instrument and experiments

Under the action of external force, coal and rock mass continuously produce cracks and release the energy stored inside in the form of electromagnetic radiation. By recording the EMR signal characteristics during the loading process of coal, the precursor information before coal mass fails can be further obtained. In this experiment, the EMR amplitude and pulse of coal mass under different loading conditions (cyclic loading and multi-stage loading) are collected and analyzed, which reflect the deformation and failure characteristics of the coal mass under complex stress environments.

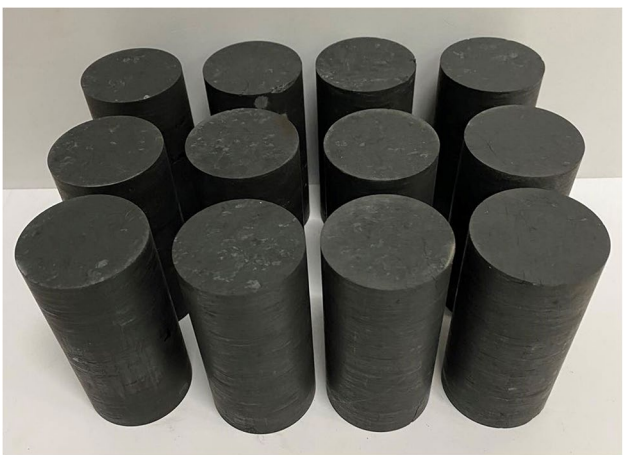

Fig. 1 Coal samples prepared for experiments

To make the loading test more stable and the test data more accurate, the test uses the loading control system and the acoustic emission test system to work in coordination with each other. This test adopts a constant velocity displacement control method, with a displacement control rate of 0.01 mm/min, to conduct a high-precision and high-stability coal body loading deformation test. The loading control system takes the Tianchen microcomputer control servo rock three-axis testing machine as the main body and is equipped with the Tenson-Test automatic control program to realize the simplification and intelligentization of the whole loading process. At the same time, the program can realize the autonomous switching of the loading control mode and can flexibly customize specific control procedures according to the actual needs of the test. The EME test system mainly includes the host, the external loop antenna and its data connection line, the antenna fixing frame, and the EME shielding network. The host of the test system adopts the EHE-HF electromagnetic radiometer produced by Beijing Century Tianzheng Technology Co., Ltd., which has an explosion-proof function. The external antenna adopts the SAS-560 passive loop antenna produced by AHSYSTEMS, with a diameter of 51/4 = 13.3 cm, a detection range of 20 Hz–2 MHz, a default sampling frequency of 10 MHz, and a resistance of 10 ohms which can adapt to the magnetic field test in different locations according to IEEE-291calibration. The EMR experimental system of loaded coal is shown in Fig. 2.

The EMR experimental methods and procedures

The Sihe standard coal samples were selected and labeled SH01 ~ SH02, which were subjected to cyclic loading and multi-stage loading experiments respectively. The experimental scheme and steps are as follows.

1. The cyclic loading displacement control rate remains unchanged at 0.01 mm/min, and the stress increase from 0 MPa to higher values. When the stress level reaches 30%, 60%, and 90%, the stress is unloaded to 7.5 MPa each time. This process resumes until the complete failure of the specimen.
2. The multi-stage loading stress is firstly increased from 0 to 1 MPa, and then increased to 1 MPa, 3 MPa, 5 MPa, 7 MPa, 9 MPa, and 11 MPa in a stepwise manner with the control rate of 0.5 MPa/s and 2 MPa stress gradient. Each stress loading level is maintained for 200 s, and the EMR amplitude and pulse of coal samples under different loading methods are collected in real time.

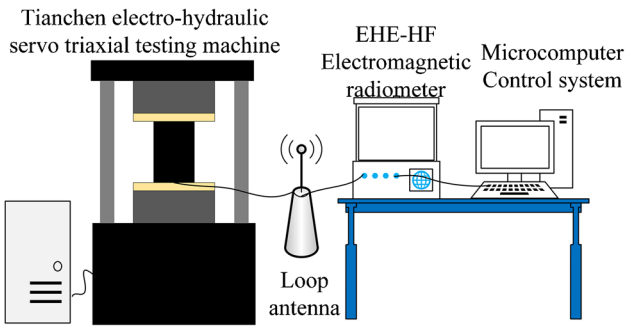

Fig. 2 The schematic of the EMR experimental system

It is worth noting that the external loop antenna needs to be set into the samples before the experiments, and the distance between the antenna and the EMR shielding network needs to be maintained throughout the experiments. After using conductive devices to ground the loading platform and samples, the whole experimental system can be covered with an EMR shielding network. Besides, to reduce electromagnetic interference from the external environments and other surrounding equipment, the laboratory doors, windows, lights, and other irrelevant electrical equipment should be closed, and prohibit people in the laboratory to walk around during the loading. To describe the research idea in this experiment more clearly and intuitively, the key nodes and steps in this experiment are shown in Fig. 3 by sorting and refining.

The initial porosity experimental scheme for coal samples

Small-angle X-ray scattering (SAXS) experiments are conducted at the BSRF 1W2A small-angle scattering station and adopted a pinhole collimation system. When the X-ray is irradiated onto the sample, if there is a nano-sized density inhomogeneous region (1 ~ 100 nm) inside the sample, some scattered X-rays will appear in the small-angle range of 2 ~ 5° around the incident X-ray (Li et al. 2014; Nie et al. 2020a, b). The coal sample is fixed on the testing platform before experiments, and the exposure time is set up at 4 s. It is worth noting that the distance from the sample to the Mar165CCD detector is 1550 mm with a detection diameter of 165 mm. Furthermore, the incident X-ray wavelength is 0.156 nm and its intensity is normalized by a calibrated ionization chamber. The schematic of the 1W2A SAXS station is shown in Fig. 4.

Experimental results and analysis

The stress–strain curves of coal under different loading conditions

The typical stress–strain curve is divided into five stages: viscoelastic phase (OA), linear elastic deformation stage

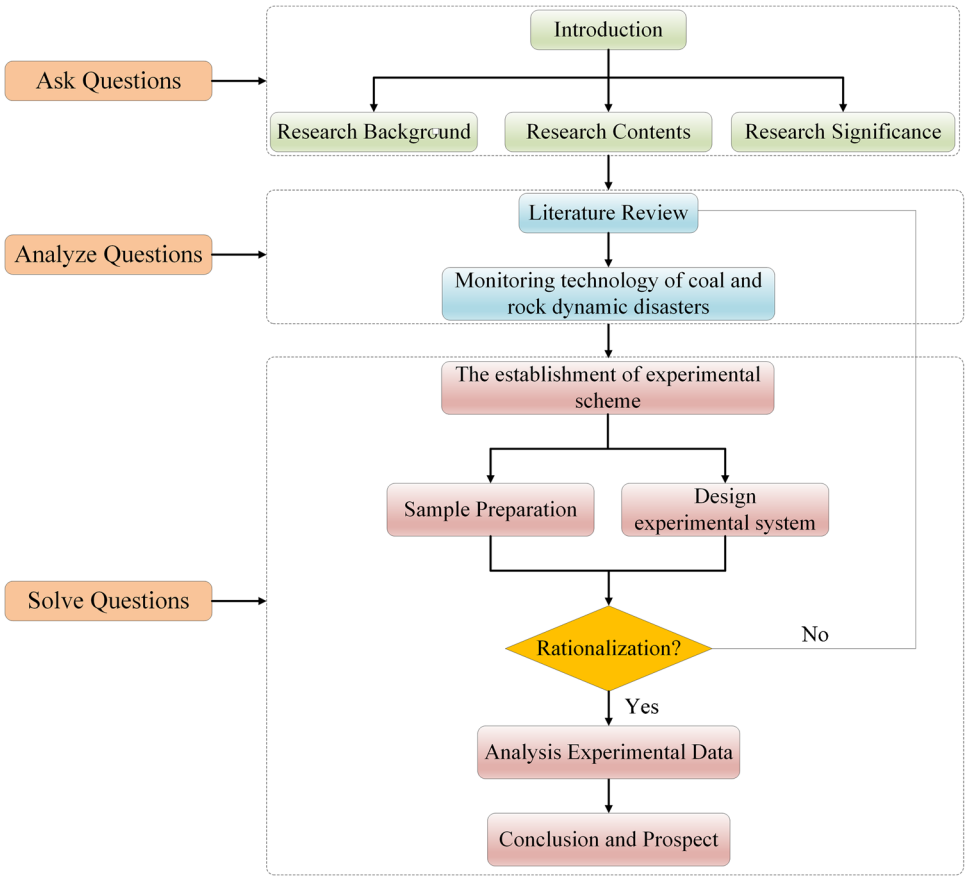

Fig. 3 The research flow chart for EMR characteristics

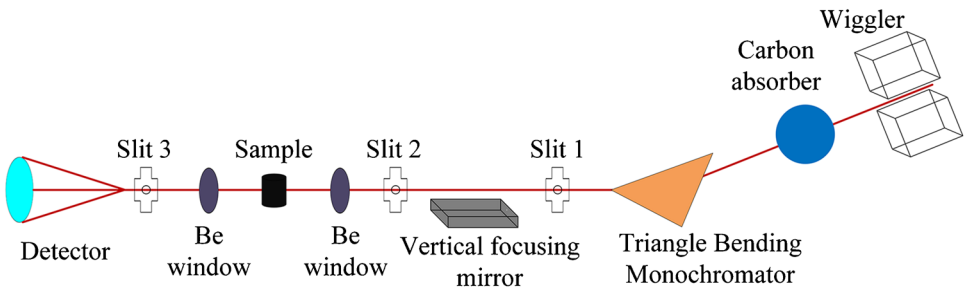

Fig. 4 The schematic of the 1W2A SAXS station

(AB), inelastic deformation stage (BC), unstable fracture expansion stage (CD), and post-peak failure stage (DE) (Pege et al. 2018; Zhang et al. 2020). All stages are associated with changes in internal defects such as cracks and pores (Su et al. 2021). The typical stress–strain curve and total stress–strain curves of the coal mass under different loading methods are shown in Fig. 5.

It can be seen from Fig. 5b that the uniaxial compressive strength (UCS) values under cyclic loading and multi-stage loading conditions are 12.12 MPa and 11.33 MPa, respectively. The mining activities in coal mines break the equilibrium state of the initial original rock stress, and the mining stress changes periodically with the engineering disturbance activities such as mining, blasting vibration, and drilling. Therefore, coal mass is in the stress environment of constant loading and unloading, which changes the deformation and failure process of loaded coal and increases the fatigue damage time of loaded coal. Finally, it will be changing the EMR characteristics during the deformation and failure process of loaded coal.

EMR characteristics of loaded coal under cyclic loading

Three groups of cyclic loading experiments were carried out this time. However, due to the limitation of the length of the manuscript, the EMR characteristics of sample SH01 are analyzed as an example. The EMR characteristics under cyclic loading conditions are shown in Fig. 6.

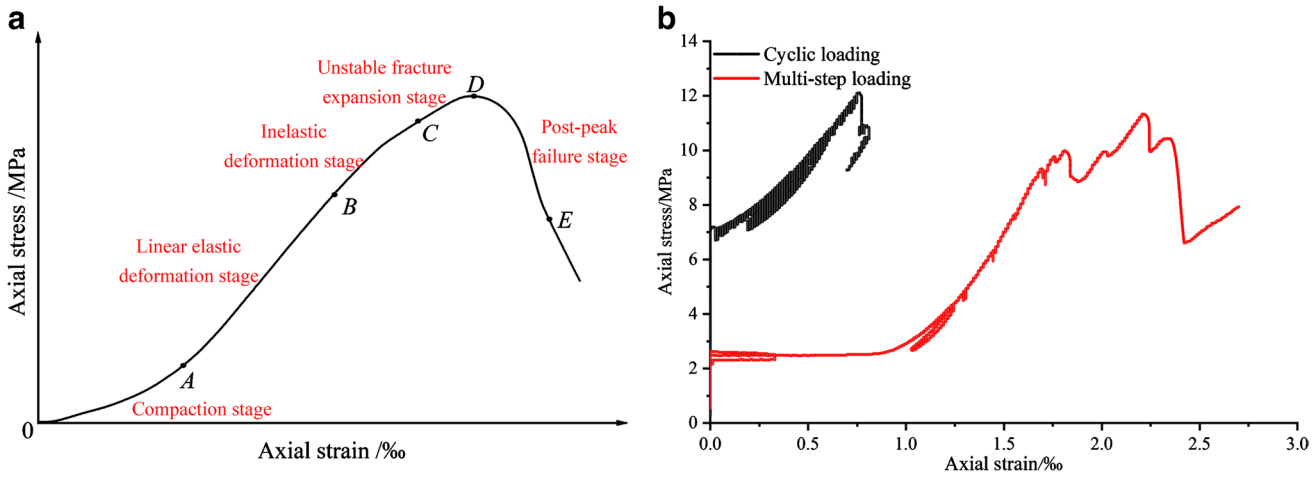

Fig. 5 The theoretical and experimental stress–strain curves of coal: (**a**) The typical stress–strain curve of coal; (**b**) The stress–strain curves of coal under different loading methods

As can be seen from Fig. 6, when the coal sample is under cyclic loading, EMR signals are generated in both loading and unloading processes. During the loading process, the EMR amplitude and pulse increase with the increase of axial load, and the number of the EMR pulse increases with the number of cycles. In addition, various fractures are compressed and closed during the loading process, and many new fractures are also generated under the action of external force. In this case, the EMR amplitude and pulse increase with the increase of the number of rupture sources. However, part of the fractures in the closed state gradually turned into the open state during the unloading process. At this time, the energy released in the coal is reduced. Therefore, the EMR amplitude decreases with the decrease of axial load. But there are still a few fractures in the unloading stage and they will be further developed, resulting in the number of the EME pulse being in a state of constant increase. When the loading time is about 500 s, the distribution of the fractures reaches the maximum inhomogeneous degree, and the EMR amplitude variation reaches the peak at this time. Moreover, when the loading time is about 725 s, the coal sample enters the unstable fracture expansion stage, which results in maximum energy release in coal, and the EMR pulse increases abruptly.

EMR characteristics of loaded coal under multi-stage loading

Three groups of multi-stage loading experiments were carried out in this phase of the research. However, due to the limitation of the length of the manuscript, the EMR characteristics of sample SH02 are analyzed as an example. The

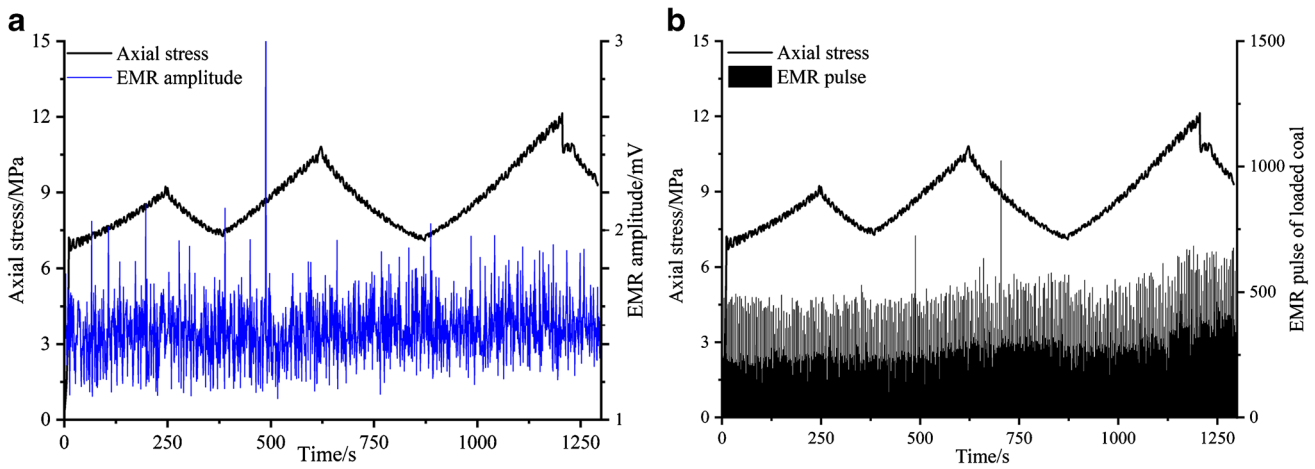

Fig. 6 EMR characteristics of loaded coal under cyclic loading: (**a**) The EMR amplitude of loaded coal; (**b**) The EMR pulse of loaded coal

EMR characteristics under multi-stage loading conditions are shown in Fig. 7.

It can be seen from Fig. 7 that when the coal is under multi-stage loading conditions, the EMR pulse and amplitude signals are generated in the whole loading process. The experimental results show that the EMR characteristics of coal samples are closely related to the loading modes. The EMR amplitude under multi-stage loading is about twice that of loaded coal under cyclic loading, while the EMR pulse number under multi-stage loading is much less than that of loaded under cyclic loading. That is because the pores, fissures, and other defective structures in the coal slowly crack and develop in the constant load stage, and produce a few new fissures, which lead to the increase in the EMR pulse number being smaller. However, during the process of interstage stress change, the development of cracks in the coal is obvious and many small cracks are produced due to the sudden change of the axial stress. Besides, the closing and opening process of pore structures is gradually accelerated, which leads to the EMR amplitude and pulse number both increasing significantly. Overall, the EMR amplitude and pulse have no obvious growth trend with the increase of axial load. Even in the 4th loading stage, that is, when the loading time is about 1150 s, the EMR amplitude and pulse even has an obvious decreased trend. However, the coal sample gradually enters the inelastic deformation and unstable fracture expansion stage with the gradual increase of interstage stress. The cracks in the coal are developed and there are many irreversible and convergent damage cracks in the coal. The energy stored in the sample is released in large quantities until the sample is completely failed. At this time, the EMR amplitude and pulse also have a noticeable growth trend.

Discussions

Quantitative analysis on the difference of EMR characteristics of loaded coal

There are three loading and unloading stages under cyclic loading conditions. In this way, the whole cycle loading experiment that includes each loading process and each unloading process can be divided into six stress stages. There are 6 interstage stress variations in total under multi-stage loading conditions. Similarly, the whole multi-stage loading experiment that includes each stress loading process can be divided into six stress stages. To reveal the difference in EMR characteristics of loaded coal under the two loading modes, the quantities of the EMR pulse generated in each stage are accumulated, and the accumulation curves of the EMR pulse with the loading stage are shown in Fig. 8.

It can be seen from Fig. 8 that the quantities of the EMR pulse generated at each stage until the coal completely failed under cyclic loading are much more than that under multi-stage loading. All the accumulation curves of the EMR pulse have a sudden increasing trend on the eve of the instability and failure of loaded coal, but also the difference between the two also reached a maximum value of 83,511. Under the cyclic loading condition, the loaded coal is in a long-term and repeatedly changing stress environment, which leads to more complex crack propagation laws and more new fractures in loaded coal due to the cycle of axial stress. Although the loaded coal is in a long-term and changing stress environment under multi-stage loading, the stabilization period of each stress level corresponds to the loaded coal being in a creep loading process, which leads to less fracture generation. Due to the loaded coal being more prone to fatigue damage, the accumulation curve of the EMR pulse

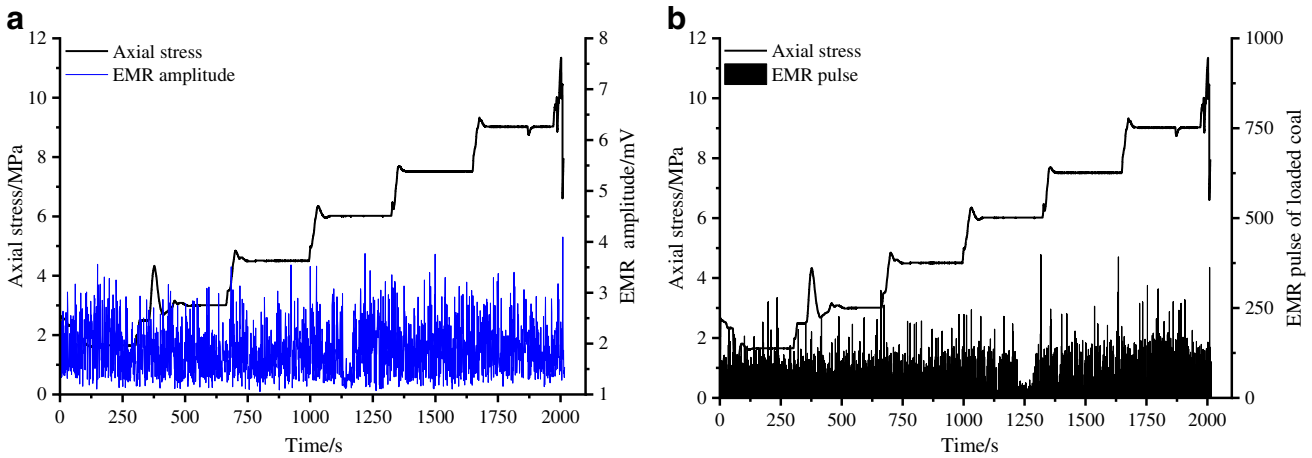

Fig. 7 EMR characteristics of loaded coal under multi-stage loading: (**a**) The EMR amplitude of loaded coal; (**b**) The EMR pulse of loaded coal

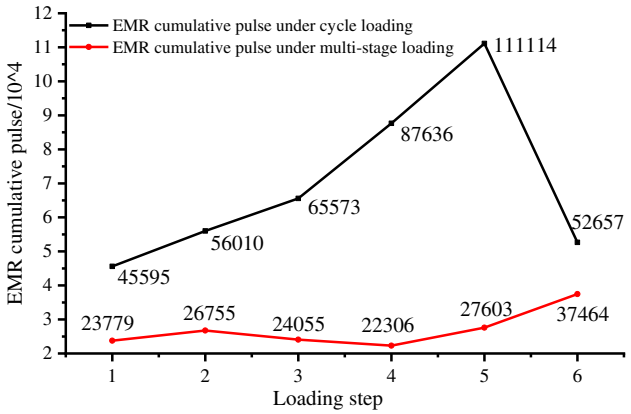

Fig. 8 The accumulation curves of the EMR pulse with the loading stage under different loading modes

with the loading stage multi-stage loading only shows up as a gentle increasing trend. To better quantify the difference in EMR characteristics of loaded coal, a more detailed description, and analysis will be given in section "The relationship between EMR characteristics and porosity of loaded coal under different loading modes."

The relationship between EMR characteristics and porosity of loaded coal under different loading modes

The volume percentage of scatterers measured by SAXS experiments is referred to as the porosity of materials. Coal is a typical porous material and its porosity can be obtained according to Eq. 1 (Li 2013; Xie et al. 2018; Zhao et al. 2018).

$$\overline{(\Delta\rho)^2}=(\Delta\rho)^2\omega(1-\omega)=\frac{1}{2\pi^2 \mathrm{V}}\int\int_0^{\infty} \mathrm{q}^2 I(q)dq \tag{1}$$

where $\Delta\rho$ is the electron density difference in $e/\left(10^{-3}nm^3\right)$, V is the radiation volume of X-ray to the sample in nm^3, and $I(q)$ is the absolute scattering intensity of the sample in PHS/s.

Under complex stress loading conditions, the quantities and types of pore structures such as micropores and mesopores in loaded coal change constantly. Various types of cracks such as modes I, II, III, and other types expand along the direction parallel to the axial stress or at a certain angle with the axial stress, and many small cracks are also derived from primary fractures (Ai et al. 2020; Liu 2019). The variation regularities between various types of pore deformation and new fractures within the loaded coal change its internal porosity situation. With the increase of axial stress, the deformation, fracture, and development of pore structures in the loaded coal go through 5 stages: viscoelastic phase (OA), linear elastic deformation stage (AB), inelastic deformation stage (BC), unstable fracture expansion stage (CD), and post-peak failure stage (DE). There is a close correlation between porosity, EMR, and axial stress in coal mass (Li et al. 2019a, b; Lou et al. 2019a, b). During the loading process, when measuring the volumetric strain of the sample (including the change of pore and fracture volume and the change of skeleton volume), the dynamic porosity during the loading can be obtained by the relationship between the initial porosity obtained from the SAXS experiment, the volume modulus, and the hydrostatic pressure (Qin et al. 2010).

$$\varepsilon_{\mathrm{v}}=\left(1+\varepsilon_{\mathrm{x}}\right)^2\left(1+\varepsilon_{\mathrm{y}}\right)-1 \tag{2}$$

where ε_{v} is the volumetric strain, ε_{x} is the transverse strain, and ε_{y} is the axial strain.

$$\eta=\frac{\eta_0-\varepsilon_v+\frac{\sigma_0}{K}}{1-\varepsilon_v} \tag{3}$$

$$\sigma_0=\frac{1}{3}\left(2\sigma_x+\sigma_{\mathrm{y}}\right) \tag{4}$$

For cyclic loading and multi-stage loading methods, the hydrostatic pressure is:

$$\sigma_0=\frac{1}{3}\sigma_{\mathrm{y}} \tag{5}$$

$$K=\frac{E_{\mathrm{m}}}{3(1-2\nu)} \tag{6}$$

where η is the porosity of the coal sample, %; η_0 is the initial porosity of the coal sample, %; K is the bulk modulus in MPa; σ_0 is the hydrostatic pressure in MPa; σ_{y} is the axial stress in MPa; E_{m} is the elastic modulus in GPa; and ν is Poisson's ratio.

The relationship between EMR pulse and porosity

The initial porosity of the Sihe coal samples is 10.25%, calculated by Eq. (1) based on the SAXS experimental results. The value of the elastic modulus is 2.5173 GPa, and the porosity and EMR variation curves under cyclic loading conditions are obtained according to Eqs. (2) ~ (6) as shown in Fig. 9.

As can be seen from the cumulative pulse counting of the EMR curve in Fig. 9, the quantity of EMR cumulative pulse increases continuously with the increase of the loading time in both loading and unloading stages. When the cycle loading process gradually proceeds to the 3rd stage, the EMR cumulative pulse counting rises fastest. When the cycle

loading process gradually proceeds to the 5th stage, that is, the axial stress increases to 85% of the uniaxial compressive strength, at this point the quantity of EMR cumulative pulse in the 5th stage also increased to a peak of 1,111,114. During the 6th loading stage, the stress–strain curve of the coal sample gradually enters the post-peak failure stage, and the quantity of EMR cumulative pulse also suddenly decreases to 52,657. Besides, Fig. 9 illustrates that the EMR cumulative pulse counting curve is consistent to maintain the growth trend in the first 5 levels of the loading and unloading processes. The increase in both the 2nd and 3rd stages is around 10,000, while the increase in both the 4th and 5th stages is more than 20,000. With the increase in loading time, the loaded coal enters into the instability fracture expansion stage, where more irreversible cracks are generated. They expand unsteadily and converge rapidly, and different forms of energy stored in the sample are released until the sample is completely failed, resulting in a significant increase in the cumulative pulse counting of EMR signals.

Figure 9 shows that the porosity change amplitude has a continuous downward trend when the axial stress gradually increases from 0 MPa to the peak stress in the first loading stage. In the first loading stage, the initial pores and fractures are compacted and the quantity of large- and medium-sized pores is decreasing. When the stress enters the 2nd stage, part of compacted pores and fractures will gradually open, expand, and develop again, and few new fractures are generated at this time. However, due to the 2nd stage being the unloading stage, the impact on the inner structures in the loaded coal is much less than the initial loading stage, so the increase in the amplitude of porosity is not evident, and the growth amplitude of EMR cumulative pulse counting is also much smaller than that in the first stage. With the progress of cyclic loading, the internal fracture sources and new fractures are constantly generated. Various types of pores and fractures are compressed and closed, which further intensifies the mutual friction between the coal matrix, and increases the amplitude of porosity and the EMR cumulative pulse counting. When the cycle loading process gradually proceeds to the 5th stage, the internal pore distribution of the coal sample tends to reach the maximum unevenness, the change degree of porosity also reaches the maximum, and the EMR cumulative pulse counting also leans to the maximum.

The relationship between EMR pulse and porosity under multi-stage loading

Similarly, the porosity and EMR variation curves under multi-stage loading conditions are obtained according to Eqs. (2) ~ (6) as shown in Fig. 10.

According to Fig. 10, the EMR cumulative pulse counting is generated under multi-stage loading. However, the curve of the EMR cumulative pulse counting does not always increase with the loading. The quantity of the EMR cumulative pulse counting has a sudden increasing trend until the 6th loading stage; at this time, the loading stress gradually increases to the peak stress and the coal sample fails. Furthermore, the curve of the EMR cumulative pulse counting increased slightly during the 2nd loading stage. When lifting the load at the 2nd loading stage, the axial stress exhibited a sudden fluctuation due to the instability of the testing machine. At this time, new fractures are generated and the curve of the EMR cumulative pulse counting manifests a rising trend. It is worth noting that the quantity of the EMR cumulative pulse counting is in the range of 22,000 to 27,000 in the first five stages of loading. The change in the amplitude of the EMR cumulative pulse counting is small, which indicates that the axial load has little effect on EMR parameters within this loading range. After the 5th loading stage, the change in the amplitude of the EMR cumulative pulse counting increases significantly until

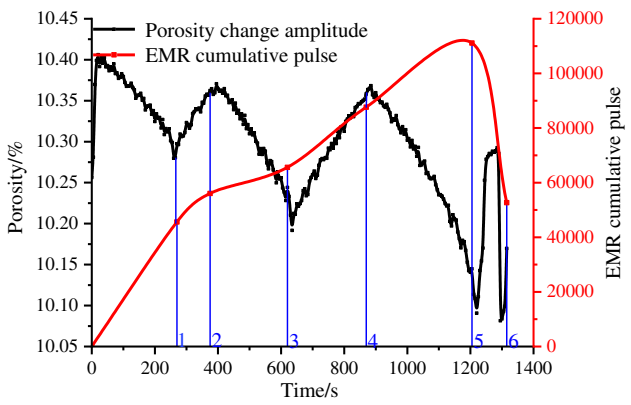

Fig. 9 The curves of the EMR cumulative pulse and porosity under cyclic loading

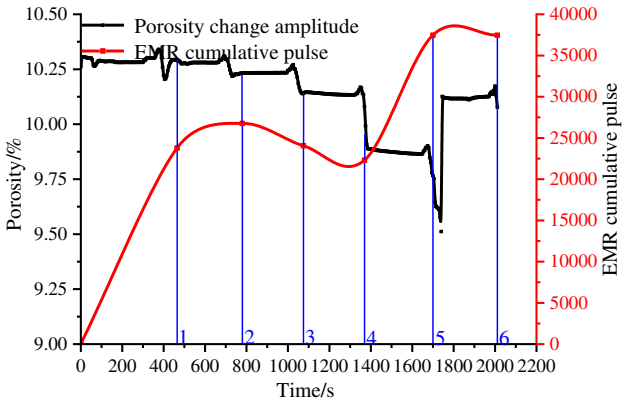

Fig. 10 The curves of the EMR cumulative pulse and porosity under multi-stage loading

the sample fails, and the quantity of the EMR cumulative pulse counting increases to 37,464. At this point, the macromain fracture is generated in the sample and more EMR signals are generated.

When the axial stress is continuously loaded at the stress levels of 1 MPa, 3 MPa, 5 MPa, 7 MPa, 9 MPa, and 11 MPa under the multi-stage loading condition, the curve of the porosity change amplitude has a continuous downward trend. Due to the relatively low-stress level in the 1st loading stage, the pores, fractures, and other crystal defect structures in the coal are hardly affected and only a few cracks are gradually compacted. At this stage, the internal structure and the porosity of the loaded coal change only slightly, resulting in a small increase in the quantity of the EMR cumulative pulse counting in the loaded coal. When the axial stress gradually increases to the 5th stage, the axial stress reaches about 9 MPa, and the internal structures of the loaded coal are gradually transformed into brittle failure. Moreover, the loading effect is equivalent to creep loading when the coal is loaded with any fixed stress level, where many large-size particles are refined, readjusted, and broken under the multi-stage loading. With the gradual increase of axial stress, the refined particles further fill the internal pores and fissure structure, and the curve of the porosity change amplitude has an increasing s-shaped downward trend due to the acceleration of particle refinement in the loaded coal. At the same time, this leads to the rapid increase of EMR pulse signals (Zhang et al. 2016, 2018). When the axial stress gradually increases to the 6th stage, the internal pore distribution of the coal sample tends to reach the maximum unevenness. At this point, the new small fractures are almost no longer generated, the porosity of the loaded coal stays at a relatively stable level, and the EMR cumulative pulse counting also leans to the maximum.

Conclusions

In this paper, the relationship between the cumulative pulse counting of EMR signals and the change of the porosity amplitude under the cyclic loading and multi-stage loading was analyzed based on EMR and SAXS experiments. The main conclusions are as follows:

1. The change of EMR pulse and amplitude in loaded coal follows the variation trend of axial stress under cyclic loading. They increase with the elevation of axial stress and decline with the decrease of axial stress.
2. The EMR pulse and amplitude of loaded coal are related to the change of loading stress level under multi-stage loading. The generation of EMR signals in the constant load stage is relatively stable, while the pulse counts of EMR signals increase during the change of interstage stress.
3. The EMR characteristics and the porosity change amplitude are related to the initiation, expansion, and derivation of fractures in the loaded coal, the changing trend of the EMR pulse counting is consistent with the curve of the porosity change amplitude, and both of them reach the maximum when the loaded is failed.

Although the EMR has been widely used in the early warning and monitoring technology of coal rock dynamic disasters, there are still several research gaps in this area. Such include enhancement of the anti-interference ability when receiving EMR signals, enhancement of the coupled prediction operation of the EMR monitoring technology and other conventional prediction methods increasing the diversity of EMR experiments in the laboratory such as loading method and failure method, and ensuring a good match between the EMR law in the laboratory and the EMR characteristics at the engineering scale. Addressing these issues in future studies could lead to the improvement of EMR warning and monitoring technology accuracy.

Acknowledgements The authors would like to thank to the staff of Sihe coal mine in Jincheng city for their help in the coring. We also would like to express our gratitude to EditSprings (https://www.editsprings.com/) for the expert linguistic services provided.

Funding This study was supported financially by the opening project of State Key Laboratory of Explosion Science and Technology (Beijing Institute of Technology) (KFJJ22-15 M), the Beijing Natural Science Foundation (8192036), and the Fundamental Research Funds for the Central Universities (2009QZ09).

Declarations

Conflict of interest The authors declare no competing interests.

References

Aydin G (2014) Production modeling in the oil and natural gas industry: an application of trend analysis. Petrol Sci Technol 32:555–564. https://doi.org/10.1080/10916466.2013.825271

Aydin G (2015) The modeling and projection of primary energy consumption by the sources. Energ Source Part B 10:67–74. https://doi.org/10.1080/15567249.2013.771716

Aydin G, Karakurt I, Aydiner K (2014) Analysis and mitigation opportunities of methane emissions from energy sector. Energ Source Part A 34:967–982. https://doi.org/10.1080/15567031003716725

Aydin G, Tarverdian S (2007) Integration of genetic algorithm, computer simulation and design of experiments for forecasting electrical energy consumption. Energ Policy 35:5229–5241. https://doi.org/10.1016/j.enpol.2007.04.020

Ai DH, Li CW, Zhao CY, Li GY (2020) Investigation on micro-seismic, electromagnetic radiation and crack propagation characteristics of coal under static loading. Rock Soil Mech 41:2043–2051. https://doi.org/10.16285/j.rsm.2019.0899

Dou LM, Wang YH, He XQ, Wang EY (2007) Study on electromagnetic emission characteristic for coal sample deformation and failure during pre-and post-peaking phases. Chin J Rock Mech Eng 05:908–914

Dou LM, He XQ, Wang EY (2004) Electromagnetic emission technique of monitoring rock burst and its application. Chin J Rock Mech Eng 04:396–399

Dou Z, Tang SX, Zhang XY, Liu RC, Zhuang C, Wang JG, Zhou ZF (2021) Influence of shear displacement on fluid flow and solute transport in a 3D rough fracture. Lithosphere-us 2021:1569736. https://doi.org/10.2113/2021/1569736

Pege G, Mineo S, Pappalardo G, Cevasco A (2018) Relation between crack initiation-damage stress thresholds and failure strength of intact rock. B Eng Geol Environ 77:709–724. https://doi.org/10.1007/s10064-017-1172-7

He XQ, Nie BS, Wang EY, Dou LM, Liu MJ, Liu ZT (2007) Electromagnetic emission forecasting technology of coal or rock dynamic disasters in mine. J China Coal Soc 01:56–59

Hu SB, Wang EY, Li ZH, Shen RX, Liu J (2014) Nonlinear dynamic characteristics of electromagnetic radiation during loading coal. J Chin Uni Min Techno 43:380–387. https://doi.org/10.13247/j.cnki.jcumt.000098

Li ZH (2013) A program for SAXS data processing and analysis. Chinese Phys C 2013:112–117. https://doi.org/10.1088/1674-1137/37/10/108002

Li ZL, He XQ, Dou LM, Wang GF, Song DZ, Lou Q (2019) Bursting failure behavior of coal and response of acoustic and electromagnetic emissions. Chin J Rock Mech Eng 38:2057–2068. https://doi.org/10.13722/j.cnki.jrme.2019.0130

Li J, Hu Q, Yu M, Li X, Hu J, Yang H (2019) Acoustic emission monitoring technology for coal and gas outburst. Energy Sci Eng 7:443–456. https://doi.org/10.1002/ese3.289

Li XS, Li QH, Hu YJ, Chen QS, Xie YL, Wang JW (2022) Study on three-dimensional dynamic stability of open-pit high slope under blasting vibration. lithosphere-us. 2022:6426550. https://doi.org/10.2113/2022/6426550

Li ZH, Wu ZH, Mo G, Xing XQ, Liu P (2014) A small-angle X-ray scattering station at Beijing Synchrotron Radiation Facility. Instrum Sci Technol 42:128–141. https://doi.org/10.1080/10739149.2013.845845

Li YA, Yin JM, Wang Y, Zhou C, Guo XF (2020) Multivariate early warning method for rockbursts based on comprehensive microseismic and electromagnetic radiation monitoring. Chin J Rock Mech Eng 42:457–466. https://doi.org/10.11779/CJGE202003007

Li J, Zhao YH, Han K, Wang Z, Wang C (2020) Electromagnetic signal characteristics and energy response pattern of briquette hammer fracturing. J Geophys Eng 17:506–516. https://doi.org/10.1093/jge/gxaa010

Liu YQ (2019) Experimental analysis of coal permeability evolution under cyclic loading. J China Coal Soc 44:2579–2588. https://doi.org/10.13225/j.cnki.jccs.2019.0353

Lou Q, He XQ, Song DZ, Li ZL, Wang AH, Sun R (2019) Time-frequency characteristics of acoustic–electric signals induced by coal fracture under uniaxial compression based on full-waveform. Chin J Eng 41:874–881. https://doi.org/10.13374/j.issn2095-9389.2019.07.005

Lou Q, Song DZ, He XQ, Li ZL, Qiu LM, Wei MH, He SQ (2019) Correlations between acoustic and electromagnetic emissions and stress drop induced by burstprone coal and rock fracture. Safety Sci 115:310–319. https://doi.org/10.1016/j.ssci.2019.02.022

Melnichenko YB, He LL, Sakurovs R, Kholodenko AL, Blach T, Mastalerz M, Radliński AP, Cheng G, Mildner DFR (2012) Accessibility of pores in coal to methane and carbon dioxide. Fuel 91:200–208. https://doi.org/10.1016/j.fuel.2011.06.026

Nie BS, Lun JY, Wang KD, Shen JS (2020a) Three-dimensional characterization of open and closed coal nanopores based on a multi-scale analysis including CO2 adsorption, mercury intrusion, low-temperature nitrogen adsorption, and small-angle X-ray scattering. Energy Sci Eng 8:2086–2099. https://doi.org/10.1002/ese3.649

Nie BS, Wang KD, Fan Y, Zhang LT, Lun JY, Zhang JB (2020b) The comparative study on the calculation of coal pore characteristics of different pore shapes based SAXS. J Min Sci Technol 5:284–290. https://doi.org/10.19606/j.cnki.jmst.2020.03.006

Qiao Z, Gao JN (2020) Research progress of electromagnetic emissions prediction technology for coal and rock fracture. Safety Coal Min 51:196–201. https://doi.org/10.13347/j.cnki.mkaq.2020.06.042

Qin YP, Wang L, Li BB, Cui LJ (2010) Change law study on porosity of the coal and rock in compression test. Min Eng Res 25:1–3

Sakurovs R, He LL, Melnichenko YB, Radlinski AP, Blach T, Lemmel H, Mildner DFR (2012) Pore size distribution and accessible pore size distribution in bituminous coals. Int J Coal Geol 100:51–64. https://doi.org/10.1016/j.coal.2012.06.005

Shen RX, Li TX, Li HR, Xue YS, He S, Hou ZH, Chen TQ (2020) Electromagnetic radiation characteristics of dry and saturated pre-cracked sandstone during fracturing. J Chin Uni Min Techno 49:636–645. https://doi.org/10.13247/j.cnki.jcumt.001168

Song DZ, Wang EY, Liu XF, Ma YK, Jin MY (2012) Correlation between electromagnetic radiation and dissipated energy of coal rock duringcyclic loading. J Chin Uni Min Techno 41:175–181

Sun Q, Liu XF, Xue L (2012) Analysis on the critical electromagnetic emission during coal or rock fracture. J Basic Sci Eng 20:1006–1013. https://doi.org/10.3969/j.issn.1005-0930.2012.06.006

Su YQ, Gong FQ, Luo S, Liu ZX. (2021) Experimental study on energy storage and dissipation characteristics of granite under two-dimensional compression with constant confining pressure. J Cent South Univ 28:848–865. https://doi.org/10.1007/s11771-021-4649-2

Wang H, Wang EY, Li ZH, Wang XR, Li DX, Ali M, Zhang QM (2020) Varying characteristics of electromagnetic radiation from coal failure during hydraulic flushing in coal seam. Arab J Geosci 13:65–74. https://doi.org/10.1007/s12517-020-05606-1

Wang Q, He MC, Li SC, Jiang ZH, Wang Y, Qin Q, Jiang B (2021) Comparative study of model tests on automatically formed roadway and gob-side entry driving in deep coal mines. Int J Min Sci Techno 31:591–601. https://doi.org/10.1016/j.ijmst.2021.04.004

Wang Y, Yang HN, Han JQ, Zhu C (2022) Effect of rock bridge length on fracture and damage modelling in granite containing hole and fissures under cyclic uniaxial increasing-amplitude decreasing-frequency (CUIADF) loads. Int J Fatigue 158:106741. https://doi.org/10.1016/j.ijfatigue.2022.106741

Wei MH, Song DZ, He XQ, Khan M, Li ZL, Qiu LM, Lou Q (2021) A three-axis antenna to measure near-field low-frequency electromagnetic radiation generated from rock fracture. Measurement 173:108563. https://doi.org/10.1016/j.measurement.2020.108563

Wei MH, Song DZ, He XQ, Li ZL, Qiu LM, Lou Z (2020) Effect of rock properties on electromagnetic radiation characteristics generated by rock fracture during uniaxial compression. Rock Mech Rock Eng 53:5223–5238. https://doi.org/10.1007/s00603-020-02216-x

Wu ZJ, Wang ZY, Fan LF, Weng L, Liu QS (2021) Micro-failure process and failure mechanism of brittle rock under uniaxial compression using continuous real-time wave velocity measurement. J Cent South Univ 28:556–571. https://doi.org/10.1007/s11771-021-4621-1

Xie F, Li Z, Li Z, Li D, Gao Y, Wang B (2018) Absolute intensity calibration and application at BSRF SAXS station. Nucl Instrum Meth A 900:64–68. https://doi.org/10.1016/j.nima.2018.05.026

Yang Z, Dai S, Li X, Qi QJ (2016) Stress-electricity-thermal coupled model of composite coal-rock in deformation and fracture under load. J China Coal Soc 41:2764–2772. https://doi.org/10.13225/j.cnki.jccs.2016.0286

Yang Z, QI Qi QJ, Xin L, Ye DD (2016) Correlation experiments with EME signals and infrared radiation of the coal-rock mixed structure in case of deformed into fractures under load. J Safety Environ 16:103–107. https://doi.org/10.13637/j.issn.1009-6094.2016.02.021

Yin S, Song DZ, Li J, He XQ, Qiu LM, Lou Q, Wei MH, Liu Y (2022) Research on electromagnetic radiation (EMR) waveform characteristics of coal failure process using Hilbert-Huang transform (HHT). Measurement 187:110195. https://doi.org/10.1016/j.measurement.2021.110195

Yuan L, Jiang YD, He XQ, Dou LM, Zhao YX, Zhao XS, Wang K, Yu Q, Lu XM, Li HC (2018) Research progress of precise risk accurate identification and monitoring early warning on typical dynamic disasters in coal mine. J China Coal Soc 43:306–318. https://doi.org/10.13225/j.cnki.jccs.2017.4151

Zhang L, Li XC, Ren TX (2020) Theoretical and experimental study of stress–strain, creep and failure mechanisms of intact coal. Rock Mech Rock Eng 53:5641–5658. https://doi.org/10.1007/s00603-020-02235-8

Zhang TJ, Shang HB, Li SG, Ren JH, Bao RY, Zhang L (2016) Permeability characteristics of broken sandstone and its stability analysis under step loading. J China Coal Soc 41:1129–1136. https://doi.org/10.13225/j.cnki.jccs.2015.0879

Zhang TJ, Shang HB, Li SG, Shi T, Pan HY, Wang Q (2018) An seepage experimental study on broken gangue under step loading during creep process. J China Coal Soc 35:188–196. https://doi.org/10.13545/j.cnki.jmse.2018.01.026

Zhao EL, Wang EY, Liu ZT, Liu XF, Jiang R (2010) Numerical simulation of electromagnetic radiation from coal or rock in a state of uniaxial compression. J Chin Uni Min Techno 39:648–651

Zhao YX, Cao B, Zhang T (2018) Experimental study on influences of permeability of axial pressures and penetrative pressures on broken rocks. J Min Sci Technol 3:434–441. https://doi.org/10.19606/j.cnki.jmst.2018.05.003

Zhu C, Karakus M, He MC, Meng QX, Shang JL, Wang Y, Yin Q (2022) Volumetric deformation and damage evolution of Tibet interbedded skarn under multistage constant-amplitude-cyclic loading. Int J Rock Mech Min 152:105066. https://doi.org/10.1016/j.ijrmms.2022.105066